MOLECULAR PHYSICS, 1990, VOL. 69, NO. 4, 639–648

Very highly excited vibrational states of LiCN using a discrete variable representation

by JAMES R. HENDERSON and JONATHAN TENNYSON
Department of Physics and Astronomy, University College London, Gower Street, London WC1E 6BT, England

(*Received 3 November 1989; accepted 28 November 1989*)

Calculations are presented for the lowest 900 vibrational ($J = 0$) states of the LiCN floppy system for a two dimensional potential energy surface (r_{CN} frozen). Most of these states lie well above the barrier separating the two linear isomers of the molecule and the point where the classical dynamics of the system becomes chaotic. Analysis of the wavefunctions of individual states in the high energy region shows that while most have an irregular nodal structure, a significant number of states appear regular—corresponding to solutions of standard, 'mode localized' hamiltonians. Motions corresponding in zero-order to Li–CN and Li–NC normal modes as well as free rotor states are identified. The distribution of level spacings is also studied and yields results in good agreement with those obtained by analysing nodal structures.

1. Introduction

Advances in both experiment and theory have led to considerable interest in the high lying ro-vibrational bound states of molecules. These states are of interest because of their unusual dynamics, compared to more familiar states with only a few quanta of vibrational energy, and because of their association with chemical reactions such as isomerization.

The LiCN molecule in particular has been the focus of many studies [1–8] of its bound state nuclear motion dynamics. All except the first of these studies employed the two-dimensional, CN bondlength frozen, SCF potential energy surface of Essers *et al.* [9], see figure 1. This surface has features which lead to interesting dynamics which is thought to be typical of many triatomic systems [5] but are encountered for LiCN at lower energies than other isomerizing systems. The surface predicts a linear LiNC absolute minimum, in agreement with experiment [10], and a metastable linear LiCN minimum at 2281 cm^{-1} above LiNC. The minima are separated by a barrier of 3455 cm^{-1} from the absolute minimum at LiNC. Classical calculations [4] show an onset of chaos approximately halfway to this barrier.

Although there has been a gradual improvement in the methods used to treat the vibrational states of LiCN, all the works cited above concentrated only on the lowest 131 states of the system. Few of these states lie above the barrier to isomerization of the system; the behaviour of the system well above this barrier thus remains an open question. It is this question that we address here.

2. Calculations

Convenient coordinates to represent LiCN are r_{CN}, here fixed at $2{\cdot}186\,a_0$, R, the distance of Li to the CN centre of mass, and θ, the angle between r_{CN} and R. θ runs from 0° for linear LiCN to 180° for linear LiNC. Bacic and Light (BL) [7] were the

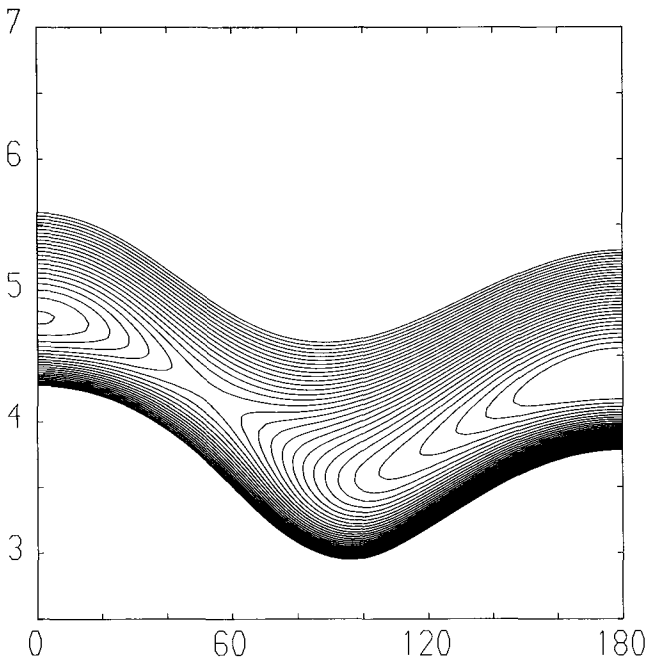

Figure 1. Contour plot of the potential energy surface for LiNC/LiCN [9]. The vertical axis gives values of R/a_0. $\theta = 0°$ corresponds to the LiCN minimum and $\theta = 180°$ to LiNC. The contours are given at intervals of $240\,\mathrm{cm}^{-1}$.

first to employ a discrete variable representation (DVR) of the θ coordinate for LiCN.

In finite basis set methods, the motion in the θ coordinate is generally carried by Legendre polynomials [2, 6] and integration in this coordinate performed analytically to give an effective radial hamiltonian [12]. In their work, BL applied a θ-coordinate transformation to this effective hamiltonian based on N_α point Gauss–Legendre quadrature. This representation, which is now discretized into N_α angles or 'rays', has formal equivalences with the untransformed problem. However, within a DVR, it is possible to diagonalize a one-dimensional radial hamiltonian for each discrete angle. BL did this using a non-orthogonal basis of distributed spherical gaussian functions for the radial coordinate.

BL then used the lowest L solutions of the one-dimensional problems to expand the full, two-dimensional problem. L, the number of solutions used to expand the final problem, can be fixed in advance or by selecting all those solutions lying below some cut-off energy, E_{RAY}. Either way, BL found that this procedure gave many more vibrational levels for less computational effort than similar calculations that used a basis set expansion for the angular coordinate.

BLs success has lead other workers, including ourselves [11], to apply the DVR method to the problem of ro-vibrational states of molecular systems. The only major difference between our approach and BLs is that for each angle we use the same set of orthogonal polynomials to carry the radial motion.

In this work we report calculations on LiCN using the surface of Essers *et al.*, see figure 1, and our DVR program [11]. These calculations give results converged with respect to basis set truncation errors for the lowest 900 vibrational (i.e. $J = 0$) states of the system. This large extension of the number of states means that infor-

mation is available for the first time on the behaviour of the system well above the barrier to isomerization.

Final calculations were performed using a DVR grid in θ based on $N_\alpha = 80$ Gauss–Legendre quadrature points. $N_R = 56$ previously optimized Morse oscillator-like functions [4] were used to diagonalize the one-dimensional hamiltonians for each of the angular quadrature points or 'rays' [7, 11]. The final hamiltonian matrix was diagonalized using the $L = 1870$ lowest of the 4480 solutions of the one-dimensional hamiltonians. This selection criterion is equivalent to choosing all solutions of the one-dimensional problem with energy less than $E_{\mathrm{RAY}} = 15231\,\mathrm{cm}^{-1}$. This basis converged the lowest 700 vibrational states of LiCN to within $0{\cdot}5\,\mathrm{cm}^{-1}$; the next 150 states were converged to 2–$5\,\mathrm{cm}^{-1}$; the highest states presented here are only converged to about $10\,\mathrm{cm}^{-1}$. Table 1 demonstrates convergence of a selection of levels with respect to changing the parameters of the calculation.

In order to analyse the results of this caculation we have plotted the wavefunctions of the lowest 900 states of the system. This method of analysing the system was used by Tennyson and Farantos [4, 5] to study the lowest 80 vibrational states of the system. They were able to characterize (*a*) regular states localized about the LiNC minimum, (*b*) regular states localized about the LiCN minimum, (*c*) irregular states localized about the LiNC minimum, (*d*) irregular delocalized states and possibly (*e*) two states which has free rotor-like character. In their work the distinction between regular and irregular states was made according to whether approximate quantum numbers could be assigned on the basis of the observed nodal structure.

The majority of our states are irregular in structure and delocalised. However inspection of our wavefunctions revealed regular states corresponding to normal

Table 1. Convergence of the LiCN band origins as a function of parameters used in the calculations. N_R gives the number of Morse oscillator-like function used for the R coordinate. N_α gives the number of discrete points used in the angular coordinate, θ. E_{RAY} gives cut-off energy for solutions of the one-dimensional radial problem in cm^{-1} relative to the LiNC minimum of the potential yielding a final hamiltonian matrix of dimension L. All band origins are given in cm^{-1} relative to the LiNC ground state at $512{\cdot}4\,\mathrm{cm}^{-1}$. Comparison of levels below level 500 show them all to be converged to within $0{\cdot}1\,\mathrm{cm}^{-1}$ by the calculations presented here.

N_R	56	56	46	51	56	56	56	56
N_α	70	80	90	90	90	80	80	80
$E_{\mathrm{RAY}}/\mathrm{cm}^{-1}$	13866	13866	14042	13950	13866	12613	13866	15231
L	1455	1661	1870	1870	1870	1470	1661	1870
Level								
500	9425·4	9425·4	9425·4	9425·4	9425·4	9425·6	9425·4	9425·3
550	9941·2	9941·2	9941·2	9941·2	9941·2	9941·3	9941·2	9941·2
600	10442·1	10442·1	10442·1	10442·1	10442·1	10443·2	10442·1	10441·9
650	10912·5	10912·4	10912·7	10912·4	10912·4	10914·4	10912·4	10912·2
700	11387·8	11387·8	11390·9	11389·4	11387·8	11390·9	11387·8	11387·2
750	11816·3	11814·6	11829·9	11815·0	11814·6	11840·2	11814·6	11813·2
800	12250·9	12250·6	12265·4	12258·6	12250·1	12322·6	12250·6	12247·4
820	12432·8	12432·5	12453·0	12432·3	12432·5	12541·7	12432·5	12430·3
840	12596·7	12597·6	12623·7	12602·3	12597·5	12732·6	12597·6	12592·2
860	12766·7	12765·6	12796·7	12773·8	12765·3	12978·6	12765·6	12758·5
880	12938·0	12982·0	12978·2	12940·8	12927·7	13205·5	12928·0	12916·3
900	13109·7	13108·7	13138·1	13113·4	13108·7	13452·8	13108·7	13086·5

modes of LiNC, normal modes of LiCN and free rotor states. These correspond to classes (*a*), (*b*) and (*e*) above. Details of these states are given in tables 2, 3 and 4 respectively. We tabulate a complete set of normal mode states as no tabulation of these appears to have been given previously. As we have only considered $J = 0$, only even quanta of bend are obtained for the quasi-linear states and only Σ free-rotor states.

Above the barrier there are very few spatially localized irregular states, such as class (*c*) above. Figures 2 to 5 show typical wavefunctions for the systems of type (*a*), (*b*), (*d*) and (*e*) respectively. These contour plots were obtained using the same

Table 2. Assignments to LiNC 'normal mode' states. States are assigned by inspection of the wavefunction (see figure 2) quanta of Li–NC stretch, v_s, and bend, v_b. States for which the nodal structures are greatly distorted are denoted by a ?.

Level No.	Frequency/ cm^{-1}	Assignments		Level No.	Frequency/ cm^{-1}	Assignments	
		v_s	v_b			v_s	v_b
1	0·0	0	0	51	2954·8	4	0
2	247·2	0	2	53	2995·5	3	10?
3	469·0	0	4	54	3025·0	0	36?
4	665·6	0	6	57	3112·8	3	12?
5	754·4	1	0	59	3188·8	4	2?
6	836·8	0	8	68	3382·0	4	4
7	982·3	0	10	75	3565·5	4	6?
8	998·1	1	2	81	3667·1	5	0
9	1111·7	0	12	91	3898·5	5	2
10	1212·8	1	4	93	3921·5	3	14?
11	1245·3	0	14	100	4083·5	5	4
12	1390·3	0	16	117	4368·9	6	0
13	1397·7	1	6	128	4597·6	6	2
14	1498·4	2	0	139	4775·9	6	4
15	1545·4	0	18	144	4874·8	6	8
16	1550·4	1	8	156	5060·1	7	0
17	1671·5	1	10	169	5286·3	7	2
18	1708·4	0	20	180	5455·0	7	4
19	1738·7	2	2	199	5740·6	8	0
20	1786·6	1	12?	213	5964·4	8	2
21	1874·8	0	22?	245	6410·6	9	0
22	1919·2	1	14?	262	6632·2	9	2
23	1946·4	2	4	272	6780·3	9	4
24	2036·8	0	24?	294	7070·0	10	0
26	2118·1	2	6	347	7718·6	11	0
28	2231·8	3	0	365	7935·9	11	2
29	2244·9	0	26?	400	8356·6	12	0
30	2246·8	2	8?	457	8984·2	13	0
32	2340·4	2	10?	515	9601·4	14	0
34	2418·2	0	28?	536	9814·7	14	2
35	2452·3	2	12?	575	10208·0	15	0
36	2469·0	3	2	598	10418·8	15	2
37	2531·3	0	30?	638	10804·4	16	0
41	2669·1	3	4	701	11390	17	0
44	2761·8	0	32?	725	11597	17	2
45	2825·4	3	6	767	11965	18	0
48	2918·3	3	8?	832	12531	19	0
49	2918·4	0	34?	900	13086	20	0

Table 3. Assignments to LiCN 'normal mode' states. States are assigned by inspection of the wavefunction (see figure 3) quanta of Li–CN stretch, v_s, and bend, v_b. States for which the nodal structures are greatly distorted are denoted by a ?. Frequencies are relative to the LiCN (0, 0) state which lies 2286·6 cm^{-1} above the LiNC (0, 0) state.

Level No.	Frequency/ cm^{-1}	Assignments		Level No.	Frequency/ cm^{-1}	Assignments	
		v_s	v_b			v_s	v_b
31	0·0	0	0	253	4229·9	5	6
40	323·0	0	2	260	4267·7	6	2
47	610·1	0	4	281	4608·8	7	0
52	689·1	1	0	284	4638·2	6	4?
58	853·7	0	6	302	4875·6	6	6
64	1016·2	1	2?	309	4963·3	7	2
76	1306·3	1	4	330	5228·8	8	0
80	1368·0	2	0	335	5271·9	7	4
88	1550·6	1	6	353	5516·6	7	6
96	1700·0	2	2	360	5585·2	8	2
111	1992·2	2	4	381	5836·9	9	0
113	2055·7	3	0	413	6199·8	9	2?
123	2234·2	2	6	433	6435·5	10	0
131	2372·4	3	2	468	6802·8	10	2
148	2666·8	3	4	489	7026·3	11	0
151	2695·6	4	0	525	7398·8	11	2
163	2912·3	3	6	545	7606·3	12	0
171	3034·7	4	2	603	8177·4	13	0
192	3345·5	5	0	663	8739·4	14	0
206	3573·4	4	6	723	9205	15	0
215	3687·7	5	2	785	9842	16	0
234	3978·5	6	0	854	10421	17	0
236	3991·2	5	4				

Table 4. Assignments to LiCN 'free rotor' states. States are assigned by inspection of the wavefunction (see figure 5) quanta of Li–CN stretch, v_s, and free rotation (or bend), m. States for which the nodal structures are greatly distorted are denoted by a ?. Frequencies are relative to the LiNC (0, 0) state.

Level No.	Frequency/ cm^{-1}	Assignments		Level No.	Frequency/ cm^{-1}	Assignments	
		v_s	m			v_s	m
65	3311·3	0	24	366	7938·3	0	53?
71	3474·8	0	26	375	8055·2	2	48?
74	3552·1	0	27?	382	8141·9	0	54
82	3671·8	0	28	399	8349·5	0	55?
87	3819·4	0	29?	409	8454·9	1	52?
94	3968·4	0	30?	459	8989·7	0	58
110	4275·1	0	33?	499	9418·6	0	60
145	4896·6	1	31?	519	9634·0	0	61?
150	4971·9	0	37?	563	10075·7	0	63
160	5139·7	1	33?	586	10299·5	0	64?
181	5468·6	0	40	609	10520·5	0	65
191	5623·3	0	41?	682	11197·5	0	66?
237	6295·2	0	45?	732	11652	0	68?
333	7539·8	0	51	783	12108	0	70?
349	7737·1	0	52	810	12337	0	73

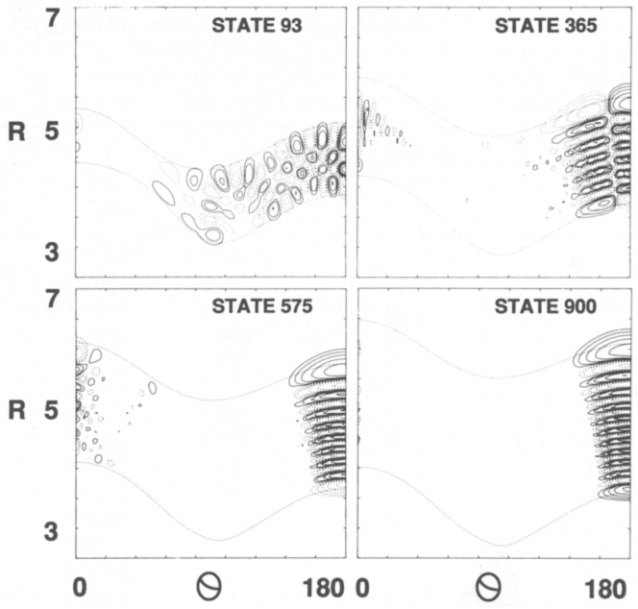

Figure 2. Contour plots of 4 typical LiNC normal mode states. Solid (dashed) contours enclose regions where the wavefunction has positive (negative) amplitude. Contours are drawn at 4, 8, 16, 32 and 64 per cent of the maximum amplitude of the wavefunction. The outer dashed contours represent the classical turning point of the potential for the associated eigenvalue.

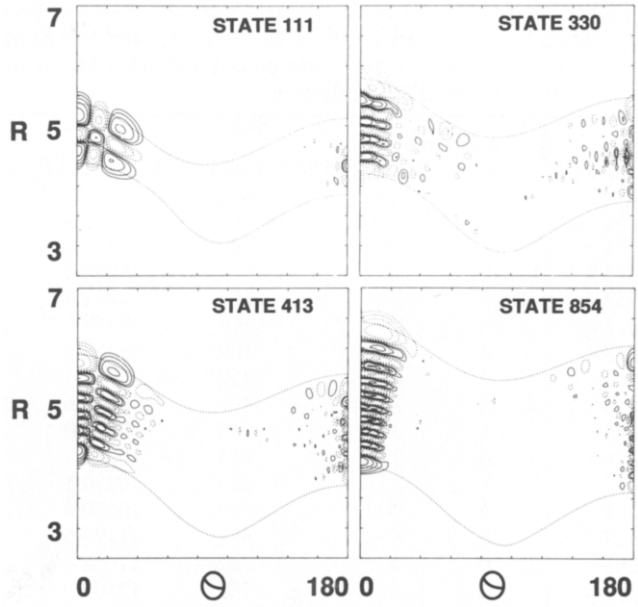

Figure 3. Contour plots of 4 typical LiCN normal mode states. Contours as in figure 2.

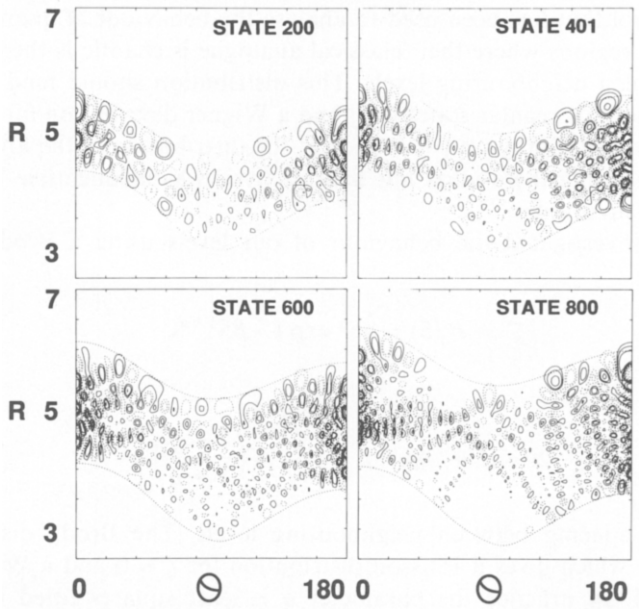

Figure 4. Contour plots of 4 typical unassignable states. Contours as in figure 2.

coordinate range as the plot of the potential, figure 1, and also have a contour denoting the classical turning point for the state in question. This allows judgements to be made about how individual wavefunctions reflect the shape of the underlying potential function and the degree to which these wavefunctions sample the available coordinate space.

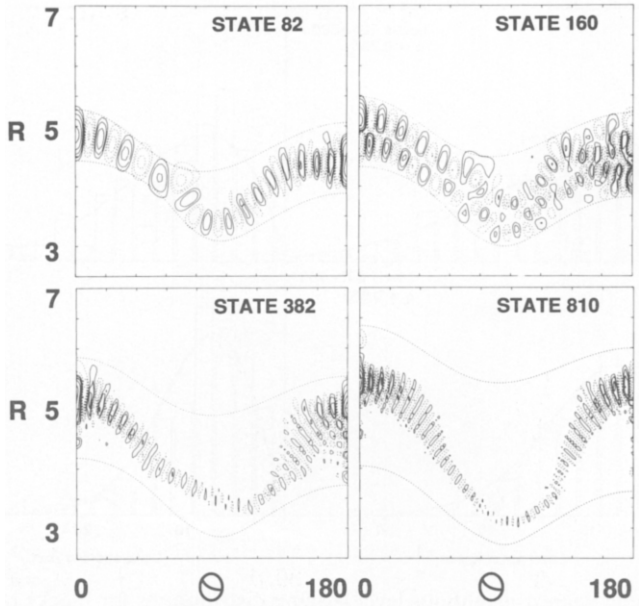

Figure 5. Contour plots of 4 typical free rotor states. controus as in figure 2.

Another tool that has been used to analyse the behaviour of quantum mechanical systems in regions where their classical analogue is chaotic is the distribution of spacings between neighbouring levels. This distribution should tend to a Poisson-type distribution for regular states [13] and a Wigner distribution for irregular ones [14]. Farantos and Tennyson [4] looked at the distribution of the lowest 80 energy levels of LiCN using these ideas but their analysis was inconclusive because of the poor statistics involved.

We have investigated the behaviour of our levels using a Brody distribution [15, 16]:

$$P_q(S) = \alpha S^q \exp(-\beta S^{1+q}), \tag{1}$$

where

$$\alpha = (1+q)\beta, \quad \beta = \left[\bar{S}^{-1}\Gamma\left(\frac{2+q}{1+q}\right)\right]^{1+q}, \tag{2}$$

and S is the spacing between neighbouring levels. The Brody distribution is a generalization which gives a Poisson distribution for $q = 0$ and a Wigner distribution for $q = 1$. In practice the parameter q is least squares fitted to the nearest neighbour distribution in question. For more details see Haller *et al.* [16].

One difficulty with our results, and we suspect with any attempt to analyse the level spacing distribution of molecules, is that the density of states increases with energy. This has a tendency to distort the idealised distributions. Although unfolding procedures have been proposed to circumvent this problem [17], we chose simply to analyse small portions of the spectrum consisting of up to 200 levels at one time. Table 5 presents a summary of the results and figure 6 shows some of the resulting distributions.

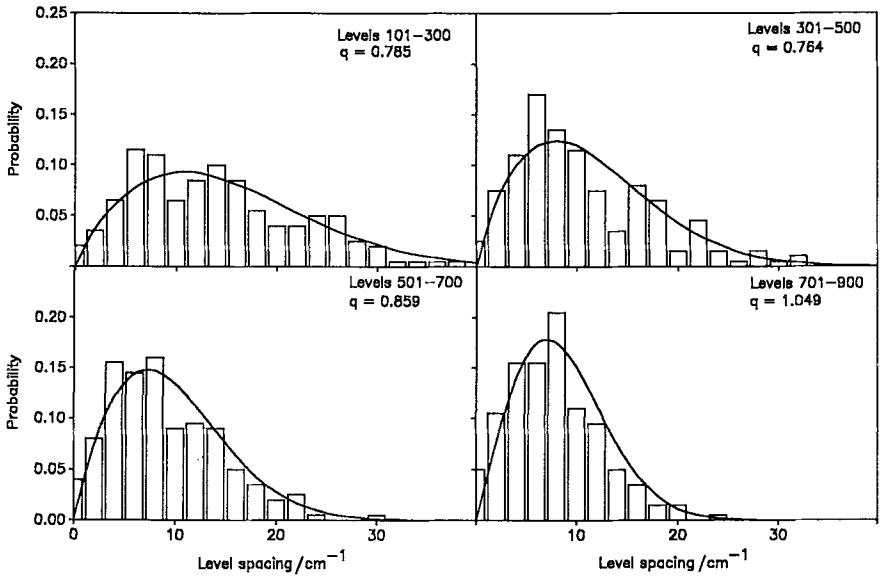

Figure 6. Sample nearest-neighbour level spacing distributions for blocks of 200 levels. The solid line is the curve given by the best fit to a Brody distribution with q as indicated.

Table 5. Level spacing distribution Brody parameter [15, 16], q, for the levels of LiCN presented here. Fits to level 101 upwards were to distributions obtained by binning the level spacings in 25 bins $2\,cm^{-1}$ wide. Levels 1–30 were placed in 12 bins of width $20\,cm^{-1}$ and levels 31–100 in 14 bins of width $5\,cm^{-1}$. The energy range of each bin is given relative to the LiNC (0, 0) state. The average level spacing, $\bar{S}$, in cm^{-1} and the standard deviation, σ, of the fit in units of probability as well as the percentage of unassigned states, u, in each fit are also given.

Levels	Energy range/cm^{-1}	$\bar{S}$	q	σ	u
1–30	0– 2240	77·5	0·154	0·034	7%
31–100	2286– 4090	26·0	0·588	0·030	44
101–300	4090– 7150	15·3	0·785	0·012	81
201–400	5768– 8358	13·0	0·798	0·015	85
301–500	7150– 9427	11·4	0·764	0·017	88
401–600	8350–10445	10·5	0·794	0·013	91
501–700	9427–11388	9·8	0·859	0·011	93
601–800	10445–12247	9·0	0·830	0·012	94
701–900	11388–13086	8·6	1·049	0·011	95

3. Discussion and conclusions

As observed [4, 5], the study of the nodal structure of the wavefunction is highly informative. In the region above the barrier we are able to identify regular states which stem from the zeroth-order hamiltonians for LiNC normal modes, LiCN normal modes and the free rotation of Li^+ about CN^-. These states should be associated with stable periodic orbits in the corresponding classical problem although free rotor periodic orbits have yet to be identified. The systematic absences in the assignable free rotor states probably correlate with energy regions where the classical free rotor periodic orbit is unstable. Similar behaviour has recently been noted in two-dimensional studies of the vibrational states of H_3^+ [18]. Another indicator that the free rotor states do not correspond to a uniform series of states is given by our failure to fit the energy levels of these states to a model free rotor hamiltonian.

Corresponding to the classically chaotic sea are the many irregular, delocalised states which are visibly ergodic in the sense that their wavefunctions sample all of coordinate space—see figure 4 for example. An estimate of the proportion of unassignable states as a function of energy is given by table 5. This shows that above the barrier to isomerization, which is reached at about state 70, only a small proportion of the states can even be approximately assigned. This change in behaviour is reflected by the Brody parameter which shows a rapid change from a near regular (Poisson) distribution for the lowest levels to a chaotic (Wigner) distribution for levels above the barrier. The use of level spacing distributions as a measure of 'quantum chaos' has proved controversial [19]. However for our results these distributions appear to give a true reflection of the underlying nature of the system.

In summary, we have used a discrete variable representation to substantially extend our knowledge of the high lying vibrational levels of the two-dimensional Li–CN system. Above the barrier to isomerization this system displays a large proportion of states that cannot be assigned. However, regular states corresponding to LiNC normal modes, LiCN normal modes and free-rotor states all exist over the entire frequency range studied.

We thank David Winstanley of the University of London Computer Centre for help in producing the graphics presented here and Dr. F. Borondo for supplying his work prior to publication.

References

[1] ISTOMIN, V. A., STEPANOV, N. F., and ZHILINSKI, B. I., 1977, *J. molec. Spectrosc.*, **67,** 265.
[2] BROCKS, G., and TENNYSON, J., 1983, *J. molec. Spectrosc.*, **99,** 263.
[3] BROCKS, G., TENNYSON, J., and VAN DER AVOIRD, A., 1984, *J. chem. Phys.*, **80,** 3223.
[4] FARANTOS, S. C., and TENNYSON, J., 1985, *J. chem. Phys.*, **82,** 800.
[5] TENNYSON, J., and FARANTOS, S. C., 1985, *Chem. Phys.*, **93,** 237.
[6] TENNYSON, J., BROCKS, G., and FARANTOS, S. C., 1986, *Chem. Phys.*, **104,** 399.
[7] BACIC, Z., and LIGHT, J. C., 1986, *J. chem. Phys.*, **85,** 4594.
[8] BENITO, R. M., BORONDO, F., KIM, J.-H., SUMPTER, B. G., and EZRA, G. S., 1989, *Chem. Phys. Lett.*, **161,** 60.
[9] ESSERS, R., TENNYSON, J., and WORMER, P. E. S., 1982, *Chem. Phys. Lett.*, **89,** 223.
[10] VAN VAALS, J. J., MEERTS, W. L., and DYMANUS, A., 1984, *Chem. Phys.*, **77,** 4061.
[11] TENNYSON, J., and HENDERSON, J. R., 1989, *J. chem. Phys.*, **91,** 3815.
[12] TENNYSON, J., and SUTCLIFFE, B. T., 1982, *J. chem. Phys.*, **77,** 4061.
[13] BERRY, M. V., and TABOR, M., 1977, *Proc. R. Soc.* A, **356,** 375.
[14] PECHUKAS, P., 1983, *Phys. Rev. Lett.*, **51,** 943.
[15] BRODY, T. A., 1973, *Nuovo Cim. Lett.*, **7,** 482.
[16] HALLER, E., KOPPEL, H., and CEDERBAUM, L. S., 1984, *Phys. Rev. Lett.*, **52,** 1665.
[17] For example: BOHIGAS, O., GIANNONI, M.-J., and SCHMIDT, C., 1986, *Quantum Chaos and Statistical Nuclear Physics*, (Lecture Notes in Physics, Vol. 263) (Springer-Verlag), p. 18.
[18] TENNYSON, J., BRASS, O., and POLLAK, E., *J. chem. Phys.* (in the press).
[19] For example: BENJAMIN, I., BUCH, V., GERBER, R. B., and LEVINE, R. D., 1984, *Chem. Phys. Lett.*, **107,** 515. MEYER, H.-D., HALLER, E., KOPPEL, H., and CEDERBAUM, L. S., 1984, *J. Phys.* A, **17,** L831.